Chemical (dis)order in a-$Si_{1-x}C_x$:H for $x<0.6$

P. I. Rovira* and F. Alvarez
Instituto de Física "Gleb Wataghin," UNICAMP, 13083, 970, Campinas, São Paulo, Brazil
(Received 28 May 1996)

We studied the local bonding structure of the hydrogenated amorphous silicon-carbon alloy system (a-$Si_{1-x}C_x$:H). The chemistry of the carbon incorporation in the alloys for $0<x<0.6$ was analyzed by infrared and visible spectroscopies. The material was deposited in a controlled atmosphere of argon and hydrogen by rf cosputtering of Si and C targets. We found that up to $x\approx 0.2$ the carbon atom prefers to bond in a chemically disordered configuration, i.e., homonuclear bonds are favored. Between $0.2<x<0.6$ a tendency to chemical ordering is apparent. These results are consistent with the behavior of the optical gap, the Urbach energy, and the density of defects of the material as a function of x. [S0163-1829(97)11807-0]

I. INTRODUCTION

In recent years quite important attempts to create good-quality a-$Si_{1-x}C_x$:H films have been made.[1] However, the different possibilities of carbon bonding make an accurate control of the deposition process difficult, leading to a material with a relatively high density of defects. There is abundant literature devoted to study the alloy deposited by plasma-enhanced chemical vapor deposition (PECVD) (Refs. 2–26) and rf sputtering (SP).[27–42] As shown in Table I, the question of the local environment of the constituent atoms of the alloy is still a matter of debate. Indeed, the understanding of the local arrangement of the atoms is important for future improvements of optical and transport properties of the material.

Chemical order, i.e., the preferred formation of heteronuclear bonds, is a characteristic feature in stoichiometric amorphous Si-C alloys. This follows from the fact that heteronuclear bonds are more stable than homonuclear bonds.[43,44] Furthermore, the rigidity of both bond lengths and bond angles of the atoms forming the alloy is a strong driving force to maximize heteronuclear bonds in a stoichiometric composition.[45] Moving away from the stoichiometric composition, a question arises as to the formation of homonuclear bonds due to effects of entropy. In past years a quite considerable number of works considered this problem, i.e., the existence of local order in the material. Let us consider a binary tetrahedrically bonded alloy $A_{1-x}B_x$ formed by a fraction $(1-x)$ and x of A and B atoms, respectively. In a *completely random* structure, the probabilities of finding A-A, B-B, and A-B bonds are x^2, $(1-x)^2$, and $2x(1-x)$, respectively. In a *completely ordered* alloy two cases are considered. For $x<0.5$, the probability of finding A-B, B-B and A-A bonds are $2x$, 0 and $(1-2x)$, respectively. For $x>0.5$, the probability of finding A-B, B-B, A-A bonds are $2(1-x)$, 0, and $2x-1$, respectively. Finally, in the case of phase separation, the probability of finding A-A and B-B bonds are $(1-x)$ and x, respectively. The structure to be favored is that which minimizes the Gibbs mixing free energy.[44] In other words, $\Delta G\approx\Delta U-T\Delta S=0$, where U and S are the formation energy and entropy, respectively. T indicates the substrate temperature, and we assumed that the variation occurs at a constant pressure, i.e., the enthalpy variation is $\Delta\mathcal{H}\approx\Delta U$. Of course, besides the substrate temperature, the presence of hydrogen is an important factor, determining the chemical and structural ordering. Indeed, H is thought to be the main cause for the poor reproducibility of alloy properties.[45]

A variety of techniques have been used to analyze the structure of the alloy. Electron spectroscopy, (e.g., x-ray photoemission, Auger, and energy-loss spectroscopies) proved to be a powerful technique to identify the bonding structure of the material. However, in order to obtain reliable information the material must be deposited and analyzed *in situ*. Indeed, a material produced *ex situ* is normally oxidized, and any attempt to determine the local bonding by that technique requires an ion milling cleaning process. In addition, ion bombardment may produce stoichiometric changes and local rearrangements of the species. Since many studies found in the literature relied on this type of cleaning procedure, the results are not so general as expected and should be revised. Raman scattering can help to identify the vibration frequencies associated with Si—Si, Si—C, C—C, and C═C bonds. Nevertheless, the photoluminescence backgrounds generally existing in the spectrum, together with the inhomogeneous linewidth, make the analysis of the spectra a difficult task. Techniques such as EXAFS (extended x-ray-absorption fine structure) and x-ray emission proved to be valuable tools to quantify the relative number of Si—C bonds. To the author's knowledge, however, most of the reported data are restricted to compositions above 20–30 C at. %.

Qualitative information about the local bonding structure is also obtained from photoluminescence (PL) experiments. The PL emission displaying a double band was interpreted by Engeman, Fisher, and Knecht[46] as being due to inhomogeneities associated with Si and C rich agglomerates. Recently, Robertson[47] suggested that the PL emission efficiency of a-$Si_{1-x}C_x$:H can be explained by assuming the existence of clusters containing sp^2 C hybrids. Experiments of nuclear magnetic resonance (NMR) by Petrich, Gleason, and Reimen[9] in PECVD a-$Si_{1-x}C_x$:H samples showed the existence of sp^2 hybrids in carbon atoms even at low carbon concentration (~10 C at. %). In addition, this technique gives information about the microstructure of the material.

Although Table I shows a diversity of results, there is

 © 1997 The American Physical Society

TABLE I. Debate about chemical order in a-$Si_{1-x}C_x$:H. The columns headed CO and CDO stand for chemical order and disorder, respectively. The column headed ''depends'' means that the authors admit both possibilities. The symbol ''+'' means that the possibility was inferred for the authors of this work. The following abbreviation have been used: SP, sputtering; GD, glow discharge; IR, infrared spectroscopy; XPS, x-ray photoemission spectroscopy; PL, photoluminescence; EXAFS, extended x-ray-absorption fine structure; AES, Auger electron spectroscopy; EELS, electron-energy-loss spectroscopy.

Deposition method	Composition	Analysis method	CO	CDO	Depends	Ref.
	$0<x<0.4$	IR, vis. spectrosc. XPS		X^+		27
	$0.6<x<1$	IR, vis. spectrosc. XPS			X^+	27
SP:Ar+Si+Graphite	$x<0.6$	XPS, H_2 effusion		X		28
	$0<x<1$	IR		X		29
	$x<0.5$	XPS, H_2 effusion	X			30
	$0.5<x$	XPS, H_2 effusion		X		30
SP: Ar+SiH_4+Graphite+H_2	$0<x<1$	XPS, IR			X^+	31
SP: Ar+Poly SiC pressed target	$x\cong 0.44$	Raman spectroscopy		X		41
GD: SiH_4+CH_4	$0.39<x<0.62$	Elect. diffraction, XPS			X	40, 22
GD: $SiH_4+CH_4+H_2$	$x=0.26$	Elect. diffraction, XPS			X	40, 22
GD: $SiH_4+CH_4+H_2$	$x=0.39$, 0.5	Elect. diffraction, XPS	X			40, 22
GD: SiH_4+CH_4	$0<x<1$	PL		X^+		2
	$x<0.7$	IR			X^+	4
	$0<x<1$	IR		X		6
	$0.2<x<0.6$	EXAFS	X			7
	$x=0.32$	EELS, Elect. diffraction	X			8
	$x<0.20$	NMR, IR		X		9
	$x<0.20$	IR		X		10
	$x<0.5$	EXAFS	X			11
	$0.5<X$	EXAFS		X		11
	$x<0.25$	Raman spectroscopy	X			12
	$x>0.5$	Raman spectroscopy		X		12
	$x<0.5$	IR	X			13
	$0.5<x$	IR		X		13
	$0.2<x<0.8$	IR			X	14
	$x<0.2$	IR	X			15
	$0.2<x<0.7$	IR		X		15
	$0<x<0.6$	XPS	X			16
	$x<0.47$	X-ray emission		X		17
	$0.47<x<0.62$	X-ray emission	X			17
	$x<0.5$	X-ray emission	X			18
	$x=0.78$	X-Ray emission		X		18
	$0<x<1$	X-Ray abs. spect.			X	19
	$0.26<x<0.6$	EXAFS	X			20
	$0<x<0.5$	visible spectroscopy	X			21
	$x=0.7$, 0.5	AES	X			25
	$x=0.25$	AES		X		25
GD: $SiH_4+C_2H_4$	$0<x<1$	IR		X		57
	$0.35<x<0.55$	XPS, AES	X			48
GD: $SiH_4+CH_4+H_2$	$x<0.35$	XPS, AES		X		48
	$x<0.5$	XPS	X			49
	$x>0.5$	XPS		X		49
	$0<X<1$	Theory		X		76
	$X=0.5$				X	23
	$0<X<1$				X	77
	$x=0.5$				X	78
	$0<X<1$				X	43
	$0<X<1$		X			44

agreement among authors about the existence of chemical order in near-stoichiometric materials. Also, there is a general agreement that in C-rich alloys there is a trend to form C═C bonds, i.e., disorded structures are promoted. In general, the conflicting results are found in studies dealing with Si-rich alloy, i.e., samples with $x<0.2$. It is evident that the strong dependence of the material structure and properties on the fabrication method conspire against a definitive answer to the question of the chemical bonding in a-$Si_{1-x}C_x$:H Therefore, in order to obtain valuable information, it is mandatory to minimize the influence of the fabrication parameters on the experimental results. A further complication is the incorporation of hydrogen. As in amorphous silicon, hydrogen plays a key role in improving the quality of the alloy by decreasing both density of defects and topological disorder.[29,48–49,50] Usually, due to the easiness of handling and deposition, most of these studies use hydrocarbon gases as carbon supply. Consequently there is a poor control of the incorporated hydrogen in the alloy. The hydrogen incorporated in samples deposited from hydrocarbon gases produces a complicated network structure as shown by the ir spectra.[51] Indeed, the spectra show the overlapping of several bands associated to C-Si, CH_n, and SiH_n, $n=1$, 2, and 3, vibration modes, preventing a clear identification of their individual contributions. This fact is a set back in the quantification of the number of Si—C bonds. The problem is partially overcome by using cosputtering of carbon and silicon targets, and also controlling the amount of hydrogen within the preparation chamber. We shall see below that the ir spectra of sputtered material are relatively easy to analyze.

In this work we address the question of preferential formation of homonuclear (chemical disorder) or heteronuclear (chemical order) bonds and its influence on the structural and optical properties of the silicon-carbon alloy. The material was prepared by SP using a gaseous mixture of argon and hydrogen. The structure was analyzed by ir spectroscopy. Photothermal deflection spectroscopy (PDS) (Ref. 52) is used to study the influence of carbon content on Urbach energy, i.e., the slope of the exponential part of the absorption coefficient, and the density of defects within the pseudogap. Using visible transmission spectroscopy, we studied the influence of carbon on the optical gap of the alloy.

II. EXPERIMENTAL PROCEDURE

Hydrogenated amorphous silicon carbon (a-$Si_{1-x}C_x$:H) films were deposited by rf cosputtering from a crystalline silicon target with a suitable amount of graphite on the top. The carbon concentration was varied by changing only the ratio between the areas of both materials. The main deposition parameters were as follows: substrate temperature 300 °C, background pressure 10^{-6} mbar, hydrogen flux 2 sccm, and target self-bias 1000 V. These conditions produce "good-quality" a-Si:H (Ref. 53) (density of defects $\sim 10^{16}$ cm^{-3}). The deposition time was around 4 h, resulting in ~ 1-μm film thickness. Before each deposition, a presputtering cleaning procedure of approximately 30 min was made on the targets. A Perkin-Elmer Fourier transform ir spectrometer in the 400–4000-cm^{-1} range was used to study the vibration spectra. Visible transmission spectroscopy was per-

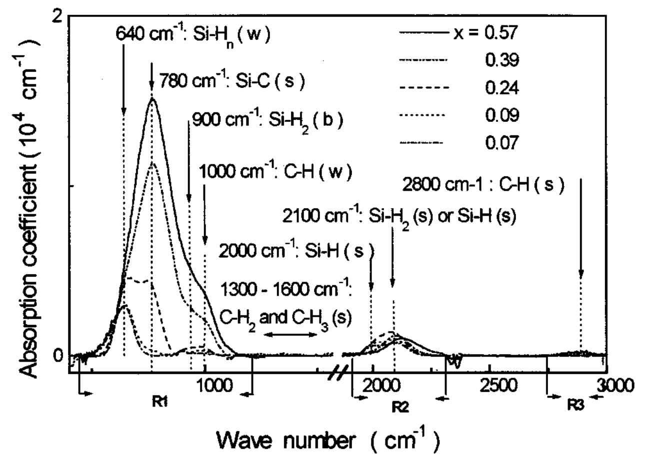

FIG. 1. Infrared-absorption spectra vs wavelength of some of the studied samples. The vibration modes are indicated by **s** (stretching) and **w** (wagging). Regions $R1$, $R2$, and $R3$ are for the purposes of discussion.

formed with a λ 9 *Perkin-Elmer* spectrometer. The optical constants and thickness were determined from the visible and infrared spectra using the Swanepoel[54] treatment. The subgap region of the absorption coefficient was determined by PDS.[52] The carbon concentration was measured by Rutherford backscattering spectroscopy (RBS).[55] Effusion experiments were used to determine the total hydrogen concentration in the films.[56]

III. RESULTS

The infrared spectra of the sample were analyzed following the standard identification of the absorption bands found in the literature.[4,6] The preference of chemical bonding is inferred from the evolution of the Si—C and Si—H vibration bands as a function of the carbon concentration. The results obtained from the visible optical spectra were used as complementary information to support the conclusions of ir spectroscopy.

A. Infrared spectroscopy

Figure 1, shows the ir spectra of some of the studied samples. In order to simplify the discussion we found it convenient to divide the ir spectra into three regions of interest, corresponding to wave numbers between 500 and 1200 cm^{-1} (region $R1$), 1900 and 2300 cm^{-1} (region $R2$), and 2750 and 3000 cm^{-1} (region $R3$).

The features associated with CH_n, $n=2$ and 3 (1300–1600-cm^{-1} range) complexes[57,58] are not visible in the ir spectra for the whole range of studied carbon content. Indeed, due to the partial cracking of the starting gases, the CH_3 and CH_2 complexes are generally found in samples deposited from mixtures containing hydrocarbon.[5,10,25,51,57–59] On the other hand, the cosputtering deposition technique uses graphite as the source of carbon atoms, making the formation of those types of complexes less probable. As we shall see below, hydrogen effusion experiments show that much less H is incorporated in sputtered material (roughly a factor 2) than in PECVD material. Moreover, the total amount of hydrocarbons like CH_4, C_2H_4, and C_3H_6, effused

from the samples is approximately 100 times smaller in sputtered material than in PECVD material, consistent with the absence of features at the 1300–1600-cm^{-1} region of the ir spectra. Therefore, from the experimental data we conclude that H bonded to C mainly forms C—H bonds, i.e., just one H attached to carbon (region $R3$, Fig. 1). The modes associated to the C—H bond are the stretching and wagging ones, located at ~2700 and ~1000 cm^{-1}, respectively.

Due to the presence of CH_n complexes in PECVD material it is somewhat controversial the assignment of the band located at 780 cm^{-1} to Si—C bonds. Conversely, in sputtered material with and without hydrogen, the 780-cm^{-1} band is identified as due exclusively to Si—C bonds.[31]

We note that the absorption band in region 1 is the sum of four contributions:[58,60,61] (1) C—H wagging (w) (~1000 cm^{-1}); (2) SiH_2 bending (b) (~900 cm^{-1}); (3) Si—C stretching (s) (~780 cm^{-1}); and (4) Si—H_n, $n=1,2,3$ wagging (w) (~640 cm^{-1}) modes, respectively.

Region 2 corresponds to the well-established stretching modes of Si—H_n ($n=1$, 2, and 3) complexes[60] (2000–2100 cm^{-1}). Furthermore, the 2000-cm^{-1} band is associated with Si—H (s), while the 2100 cm^{-1} is associated with Si—H_2 and Si—H (s) vibrations located on internal surfaces (voids).[56]

Now, we proceed to describe the method used for the determination of the relative number of Si—C bonds as a function of C content. As remarked above, the absorption band in region $R1$ (Fig. 1) is due to four contributions with quite well-identified positions. These are associated with C—H (w), SiH_2 (b), Si—C (s), and Si—H_n (w), $n=1$, 2, and 3 modes, and the area below each band is proportional to the number of the corresponding oscillators. The individual contributions to the total band are obtained by fitting four Gaussians centered at 780, 640, 900, and 1000 cm^{-1}, respectively. We note that in the fitting processes only the positions of the Gaussians were fixed. To confirm the reliability of this deconvolution we applied a second procedure involving the integration of the stretching SiH_n modes. The details of this method are given in the Appendix. Figure 2 shows the normalized area of the absorption bands associated to Si—C bonds as a function of C content. The open circles correspond to the straightforward deconvolution process and the method is reliable for spectra with quite well-resolved bands. The open triangles correspond to the second method and it assumes that the total number of Si—H (w) oscillators is proportional to the total number of Si—H (s) oscillators (see the Appendix).

Figure 3(a) shows the H atoms bonded to Si as a function of carbon concentration, as determined by integration of the Si—H_n (s) modes (see the Appendix). The concentration of H bonded to C was determined by integration of the band associated to the stretching mode of C—H (s) bond (region $R3$, Fig. 1). To convert from the oscillator strength to atomic concentration, we used the value ~1.7×10^{21} cm^{-2} for the proportionality factor [Fig. 3(b)].[62] As we do not know the density of the films, we have used an averaged value between densities of C and Si. It should be pointed out that the absolute value of the H concentration shown in Fig. 3 must be cautiously considered because of the uncertainty involved in the experimental determination of the proportionality factor and density of the material. However, experiments of H

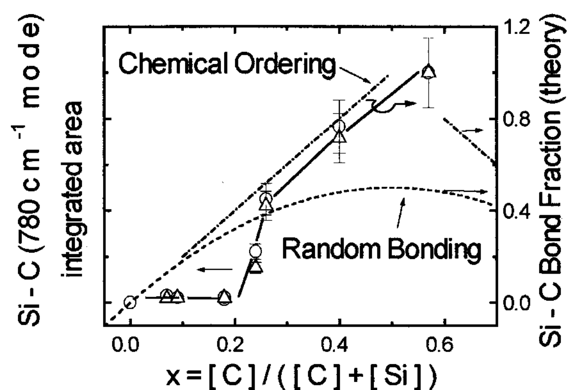

FIG. 2. Integrated area of the Si-C band (arbitrary units) vs the compositional parameter, $x=[C]/([C]+[Si])$. Open circles: direct deconvolution of absorption bands from Fig. 1. Open triangles: indirect method involving the Si-H (s) band. The experimental data were fitted assuming chemical ordering for the near-stoichiometric material ($x\approx0.57$). The full lines are guides for the eyes. The dashed-dotted and dashed lines are theoretical curves corresponding to chemical ordering and random bonding structures, respectively.

effusion support these estimations. Figure 3(c), open triangles, shows the total H concentration obtained by effusion experiments as a function of the composition parameter x. The open squares were obtained by summing the values indicated in Figs. 3(a) and 3(b). Therefore, the good agreement of both results suggests that the fraction of Si—H and C—H bonds are well estimated.

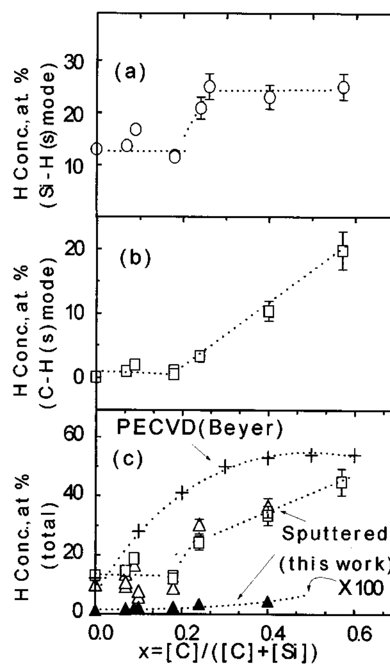

FIG. 3. (a) H at. % bonded to Si (from ir results) vs the compositional parameter x. (b) H at. % bonded to C (from ir results) vs the compositional parameter x. (c) Empty squares: total amount of H obtained by summing values from (a) and (b). Empty triangles: total amount of H obtained by effusion experiments. Filled triangles: total amount of hydrocarbons effused from sputtered samples. For comparison purposes we plotted the total amount of H effused from PECVD samples (crosses, Ref. 56). The dashed lines are guides for the eyes.

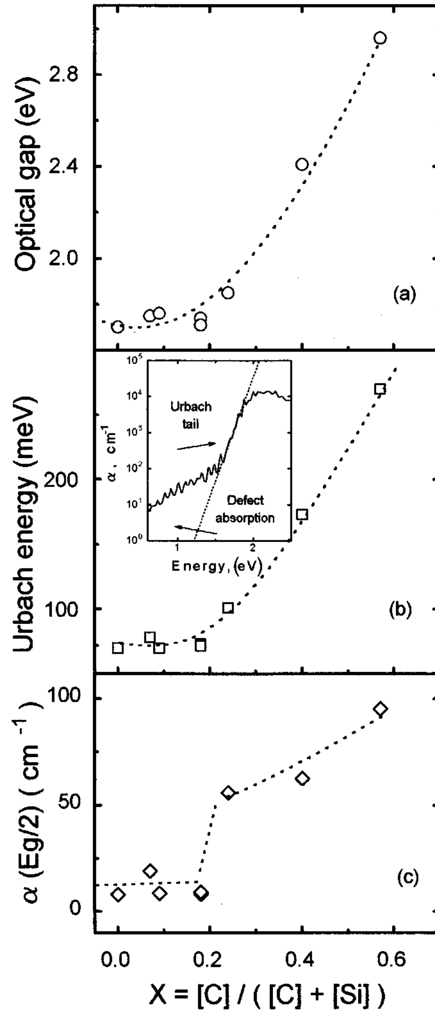

FIG. 4. (a) Optical gap (Tauc) vs the compositional parameter x=[C]/([C]+[Si]), (b) Urbach energy vs the compositional parameter x. The dashed lines are guides for the eyes. Inset: Typical subgap absorption spectrum. (c) Absorption coefficient at the midgap value α ($E_g/2$) vs compositional parameter x. The dashed lines are guides for the eyes.

B. Visible spectroscopy

The optical gap and the Urbach energy as a function of x are shown in Figs. 4(a) and 4(b), respectively. Following the procedure of Tauc (see, for instance, Mott and Davis[63]), the optical gap was obtained from the extrapolation to zero absorption of the quantity $(h\nu\alpha)^{1/2}$ versus $h\nu$. Here $h\nu$ is the photon energy, and α is the absorption coefficient. The Urbach energy is defined as the slope of the exponential part of the absorption coefficient [Fig. 4(b), inset].

In amorphous semiconductors, the area under the subgap absorption coefficient is proportional to the total density of defects of the material. Usually, this area is defined by subtracting from the total area under the absorption coefficient, the area under the extrapolated Urbach edge (tail) [Fig. 4(b), inset]. In hydrogenated amorphous silicon the absolute density of defects is obtained by electron-spin resonance, which measures the total concentration of neutral Si dangling bonds. Assuming that the dangling bond is the only possible defect, the area under the subgap absorption curve can be calibrated in density of defects.[40] In a-$Si_{1-x}C_x$:H alloys, additional complications arise due to the possibilities of both Si and C dangling bonds. In addition, we remark that the calibration procedure assumes that the Urbach tail is sufficiently steeped. Indeed, in alloys having larger Urbach energy, the procedure gives rise to misleading results since they over estimate the density of states under the Urbach energy [Fig. 4(b), inset]. In order to avoid these ambiguities, we shall compare the absorption coefficient α for different samples evaluated at a photon energy equal to half of the energy gap, i.e., $\alpha(Eg/2)$. This magnitude is related to the density of defects and allows a comparison of the evolution of the alloy as a function of carbon content. Figure 4(c) represents this magnitude as a function of x.

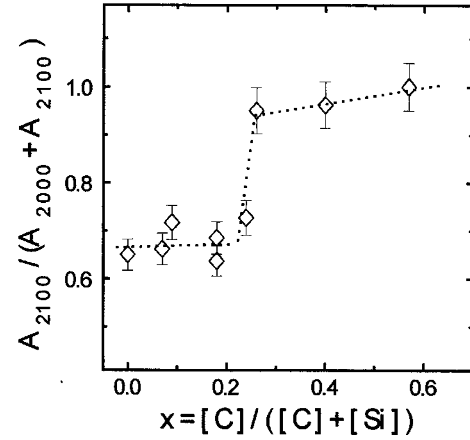

FIG. 5. Relationship between the areas of the stretching modes of the SiH_n bonds vs the compositional parameter x.

IV. DISCUSSION

We begin the discussion analyzing the behavior of the relative number of Si—C bonds as a function of x. Two important features are noted in Fig. 2: (1) up to $x\sim20$ C at. %, the concentration of Si—C bonds is small and fairly constant; (2) above $x\sim20$ C at. %, this concentration increases abruptly. This observation suggest that up to $x\sim20$ C at. % carbon atoms tend to form homonuclear bonds (chemical disorder). Above $x\sim20$ C at. %, however, carbon atoms tend to form heteronuclear bonds, an indication of a tendency towards chemical order in the alloy.

There are other effects produced by the inclusion of C. Indeed, increasing the concentration of Si—C bonds induces the formation of higher-order hydrides associated to hydrogen bonded to internal surfaces (voids).[56] This can be concluded by studying the behavior of the ratio $R=(A_{2100})/(A_{2000}+A_{2100})$ as a function of C content (Fig. 5). Here A_{2100} and A_{2000} stand for the integrated areas of the absorption bands associated with 2100- and 2000-cm^{-1} Si-H (s) vibration modes, respectively. Therefore, the step observed in Fig. 5 is probably due to an increasing density of voids. The behavior of the concentration of H atoms bonded to Si with increasing x also supports these arguments. Figure 3(a) shows a step of the concentration of H atoms bonded to Si as a function of the C concentration. This plot indicates that the step in R is also accompanied by an increasing H concentration, a characteristic feature of a less compact material.[56]

Figure 4(a) shows that the Tauc's optical gap as a function of the carbon content is approximately constant up to $x\approx0.2$. This constancy of the optical gap is consistent with homonuclear bonds, probably graphitelike bonds. Quite different is the behavior of the alloy for $x>0.2$ where the optical gap increases abruptly. As suggested from Fig. 3(a), this behavior could be partially due to excess H attached to Si. However, above $x\approx0.2$ the H contents stabilize at ~20–25 at. % whereas the optical gap increases. A comparison with PECVD material helps support on premise that the increasing optical gap is not mainly due to H. In this material, H is easily incorporated and, even at H concentration as high as ~30 at. %, the optical gap of a-$Si_{1-x}C_x$:H does not exceed ~2.25 eV.[64]

The concentration of H attached to C behaves differently. Figure 3(b) shows that up to $x\sim0.2$ this concentration is low and fairly constant, increasing monotonically for larger x values. Therefore, part of the increasing optical gap could be due to the increasing number of H atoms attached to C. As in the case of H bonded to Si, high concentrations of H alone cannot account for the measured large gaps. In fact, in PECVD material, concentrations of H bonded to C as high as 35–40 % produce a-$Si_{1-x}C_x$:H with optical gaps not larger than ~2.6 eV.[65]

There are also more fundamental physical reasons supporting these assumptions. The character of the top of the valence band in silicon-rich alloys is given by Si p orbitals.[66] In a-Si a maximum recession of the top of valence band upon hydrogenation is ~0.7 eV. Therefore, the large gap obtained in our samples cannot be explained only by the substitution of Si—Si bonds by Si—H bonds. Moreover, Fig. 3(a) shows that H attached to Si is approximately constant above $x\sim0.2$, while the optical gap monotonically augment as a function of C content. In carbon-rich alloys, photoemission experiments show that there are no induced states at the top of the valence band due to C—H bonds.[67–69] These results are corroborated by experiments of total hydrogen effusion by Fang and Ley.[66] These authors found no changes in the top of the valence band in carbon-rich samples after effusion of all the hydrogen contained in the material.

From this discussion, we conclude that the main cause of the increasing optical gaps is the increasing number of the strong Si—C bonds. We remark that some previous works report this behavior for the optical gap of PECVD- and SP-deposited materials.[9,21,27,65] However, most of these studies reported materials where the gap increases monotonically on carbon content for $0<x<0.6$.[70]

For comparison purposes, in Fig. 3(c) (crosses) we plotted the total amount of H evolving from PECVD samples reported by Robertson[43] and Beyer.[56] This plot clearly shows that, for the same amount of carbon, much less H is incorporated into the sputtered material. The filled triangles in Fig. 3(c) correspond to the sum of the effused species like CH_4, C_2H_4, and C_3H_6. We note that in PECVD material the amount of those species is approximately 100 times greater.[56] Indeed, as remarked above, PECVD material is deposited from gases like CH_4, and much more H is incorporated as polymeric fragments.

Now we proceed to analyze the evolution of Urbach energy as a function of carbon content [Fig. 4(b)]. The increasing value of Urbach energy has been associated with potential fluctuations from either the C potential or the formation of a polymeric phase.[16,43,71] According to De Seta *et al.*, at low carbon concentration the inclusion of C in the network causes strong fluctuations at the top of the valence band, increasing the disorder.[72] Indeed, the large difference of Si—C and Si—Si bond lengths causes a local stress inducing potential fluctuations. The polymeric phase is a consequence of the large amount of H incorporated into the alloy. As discussed above, however, our studied alloy does not present the polymeric phases, i.e., CH_3 complexes are absent along the whole range of the x value analyzed. Furthermore, only above $x\approx0.2$, is H substantially attached to carbon, forming C—H bonds [Fig. 3(b)]. Therefore, up to $x\sim0.2$, the invariance of the Urbach tail is consistent with the absence of both Si—C bonds and a polymeric phase. On the other hand, the substantial increase of the Urbach energy above $x\approx0.2$ could be attributed to increasing Si—C, i.e., local potential fluctuations associated with C incorporated in the network.

Figure 4(c) shows that for $x>0.2$, α $(Eg/2)$ increases as a function of x, indicating that the density of defects is increasing. This behavior is consistent with the weak-bond-to-defect conversion model of Stutzman.[73] This model assumes that the tail states are due to weak bonds and some of them can convert to dangling bonds. Therefore, materials with larger Urbach energy will have a greater tendency to convert weak bonds to defects. As shown in Fig. 4(b), the Urbach tail of the studied alloy increases substantially above $x\sim0.2$, and so does the density of defects [Fig. 4(c)], as proposed by the model.

To summarize, we conclude that for relatively low C content ($x<0.2$) the alloy is chemically disordered, i.e., homonuclear bonds are preferentially formed. At higher C concentration ($0.2<x<0.6$) the alloy is more chemically ordered, i.e., Si—C heteronuclear bonds are preferentially formed. It is interesting that direct measures of the Si—C bonds in material deposited by PECVD show comparable results. For instance, EXAFS experiments by Pascarelli *et al.*[7] in plasma-deposited a-$Si_{1-x}C_x$:H show a noticeable increase in the number of Si—C bonds above $x\approx0.25$–0.3. Similar conclusions were obtained by Robertson[43] using the Si x-ray emission spectra obtained by Weich *et al.*[18] in PECVD material. In this type of material, only above $x\approx0.35$ does the concentration of Si—C bonding begin to increase, reaching a maximum at $x\approx0.5$.[48]

These are surprising conclusions. Indeed, one can expect that, at low x, the formation of C—C bonds is improbable. Moreover, as heteronuclear bonds are more stable than homonuclear bonds,[43] Si—C bonds are more likely to form than C graphitelike bonds. It is possible, also, to imagine that the invariance of the Si—C bond concentration for $x<0.2$ stems from the fabrication method (Fig. 2). Indeed, an explanation of the existence of C—C bonds could be the incorporation of graphitelike species extracted from the target during the sputtering process. However, the abrupt increasing observed above $x\approx0.25$ indicates that basic properties related to local equilibrium during the fabrication process probably determine the final structure of the material. Therefore, we should mention some qualitative points to keep in mind when attempting to explain the experimental results.

First of all, we note that there are two dominant processes: chemical ordering, which favors the formation of het-

eronuclear bonds, and chemical disordering, which corresponds to the formation of both homonuclear and heteronuclear bonds. Near stoichiometry, chemical ordering dominates because the rigidity of bonds,[45] and also, because heteronuclear bonds are more stable than homonuclear bonds.[43,44] For a low carbon concentration, entropy effects could dominate, suggesting the possibility of homonuclear bond formation. Finally, it is interesting to remark that the observed extremely low solubility of C in Si is consistent with this suggestion. Indeed, even at the melting point of Si, the solubility of C is about 10^{-6} at. %.[74]

A last comment about hydrogen incorporation. It is worth noting that strict energetic arguments are not sufficient to explain the present experimental findings. Indeed, although the C—H bond is stronger than the Si—H bond,[44] H seems to attach preferentially to Si up to up to $x \approx 0.2$. Only when the concentration $x \approx 0.2$ is reached do the C—H bonds increase considerably [Fig. 3(b)]. This result suggests that entropy effects are important in determining the chemical bonding and should be considered. For purposes of comparison, we note that the evolution of the absorption band associated to C—H bonds has the same behavior as for the case of the alloy deposited from hydrocarbons by PECVD.[6] Therefore, we suggest that this is an intrinsic property of the alloy rather that a consequence of the fabrication method.

Now we shall compare the experimental findings with theoretical models discussed in Sec. I. Figure 2 shows the experimental integrated area (arbitrary units) of the Si-C bond as a function of the carbon concentration. This area is proportional to the total number of Si—C bonds. The experimental data were fitted assuming chemical ordering for the near stoichiometric material, i.e., the Si—C bond fraction is assumed equal to one for the $x=0.57$ sample. Indeed, for hydrogenated material, chemical ordering is expected at $x \approx 0.6$.[43] As observed in Fig. 2, the random tetrahedrically structure model (dashed line) does not reproduce at all the experimental dependence of the Si—C bond fraction against carbon concentration. Conversely, above $x \sim 0.2$ there is a reasonably agreement with the chemically ordered bonding model (dashed-dotted line). Therefore, these results suggest that for $x > 0.2$ as well, forming the ordered network minimize the Gibbs energy, favoring the development of heteronuclear bonds. For $0 < x < 0.2$, the small absolute value of the integrated area of Si—C band (Fig. 1) and its invariance on carbon content (Fig. 2), raise the possibility of phase separation. Indeed, as noted in Sec. I Robertson suggested the existence of sp^2 hybrids due to C clusters in the material.[47]

We close this section with a comment about the conflicting literature results compiled in Table I. The contradictory opinions about the existence or not of chemical order suggests that the preparation method is of primordial importance in the determination of local atomic arrangements. In particular, hydrogen is expected to play an essential role in this context. Furthermore, for alloys prepared from hydrocarbon gases, the different plasma conditions produce a diversity of hydrogenated carbon fragments, strongly determining the C coordination in the alloy. Therefore, more work on the alloy deposited by sputtering varying the amount of hydrogen can help to understand the intrinsic problem of the local coordination.

V. CONCLUSIONS

The relative number of Si—C, Si—H, and C—H bonds as a function of carbon concentration of sputtered $a\text{-Si}_{1-x}\text{C}_x\text{H}$ was inferred from infrared spectroscopy. The evolution of the optical gap, the Urbach energy, and the absorption coefficient at the midgap as a function of carbon concentration was determined by visible spectroscopy. Up to $x \approx 0.2$, the relative number of Si—C bonds, the optical gap, the midgap absorption coefficient, and the Urbach energy are approximately constant. Above $x \approx 0.2$ there is an increasing number of Si—C bonds leading to an increase of the optical gap, the midgap absorption coefficient, and the Urbach energy. For low carbon concentration, hydrogen is mainly attached to Si. Above $x \approx 0.2$ there is an increasing number of H atoms bonded to both, C and Si atoms.

The following are the main conclusions accomplished from this work.

(1) For $0 < x < 0.2$, the alloy is found to be chemically disordered; i.e., homonuclear bonds are preferentially formed.

(2) For $0.2 < x < 0.6$ there is a trend to increasing order, i.e., heteronuclear bonds are preferentially formed. In this range of x, the relative number of Si—C bonds is consistent with a theoretical model which assume a completely ordered structure.

At near-stoichiometry composition, the formation of a chemically ordered structure is energetically more favorable that a randomly structure. At low C concentration, the opposite is probably true.

ACKNOWLEDGMENTS

We are indebted to D. Comedi, R. Zanatta, and I. Chambouleyron for a critical reading of the manuscript, and to R. Carius for his interesting comments about the work. Also, we thank M. Tabacniks, IBM Almadem Research Laboratory, and W. Beyer, Institut fur Schicht-und lonentechnick, Julich, Germany, for the RBS and effusion measurements, respectively. This work was partially sponsored by FAPESP (91/3635-6 and 95/3832-7), Programa Apoio Desenvolvimento Cientifico Tecnologico, and European Union (C11*-CT93-0062). F.A. and P.I.R. are supported by CNPq and CAPES, respectively.

APPENDIX

In this appendix we shall describe a procedure used to estimate the relative Si—C bond concentrations. This is an alternative method to the straightforward mathematical deconvolution of the absorption bands.

Figure 1 shows that up to $x \approx 0.24$ the total absorption in region $R1$ has two clearly resolved contributions, namely (a) the absorption due to SiH_n (w) ($\sim 640\ \text{cm}^{-1}$) plus Si—C (s) ($\sim 780\ \text{cm}^{-1}$) modes, and (b) the absorption due to C—H (w) ($\sim 1000\ \text{cm}^{-1}$) plus SiH_2 (b) ($\sim 900\ \text{cm}^{-1}$) modes. Therefore, in order to obtain the contribution to (a) due to Si—C bonds, it is necessary to evaluate the SiH_n (w) contribution to this band.

In order to do this task we note that Langford *et al.*[75] showed that the total hydrogen concentration N_{H}, can be determined by integrating either the Si—H (s) ($\sim 2000\ \text{cm}^{-1}$) or the Si—H ($w$) ($\sim 640\ \text{cm}^{-1}$) absorption bands.

These authors studied a large number of experimental data, and found quite a good correlation between the total number of oscillators obtained from the integration of any of these bands. In that case, the total hydrogen concentration is

$$N_H = K_{640} I_{640} = K_{2000} I_{2000} + K_{2100} I_{2100}, \quad \text{(A1)}$$

where the K's and I's indicate proportionality factors and the integrated areas under the corresponding absorption bands, respectively. From Eq. (A1), I_{640} is easily obtained provided that the K factors are known. Therefore, the contribution of the Si—C bonds to the 780-cm^{-1} absorption band is estimated by subtracting I_{640} from the total area under this region. The constants $K_{2000}=(9\pm1)\times10^{19}$ cm^{-2}, $K_{2100}=(2.2\pm0.2)\times10^{20}$ cm^{-2}, and $K_{640}=(2.1\pm0.2)\times10^{19}$ cm^{-2} used in the calculation are from Langford *et al.*[75]

Now, we proceed to determine the Si—C bond density in samples with $x>0.24$. Above this value of C concentration, the bands corresponding to contributions (a) and (b) are not resolved. Then we proceed by two steps. First, we separate the contributions due to (a) and (b) by fitting two Gaussians. The Gaussians are located at ~640–780 and at ~900–1000 cm^{-1}. Next, we obtain the Si—C bond concentration repeating the procedure used for $x<0.2$.

As remarked above, this method is useful if the absorption bands are not quite well resolved and a deconvolution treatment is not straightforward. Nevertheless, the dispersion of the experimental data leading to Eq. (A1) suggests caution in the absolute values of the number of Si—C oscillators obtained from this procedure. However, Fig. 2 shows a quite good agreement of the normalized number of Si—C bonds as determined from both methods, giving confidence about the results.

Before leaving this appendix, let us to do a comment about the Si—H (s) mode of the more carbonated sample ($x=0.57$). It is noted that the Si—H (s) band shifts to ~2140 cm^{-1}. This is associated with vibrations of Si—H_n complexes ''back bonded'' to carbon.[35] To our knowledge there is not a reported proportionality factor between the area under the band corresponding to this vibration mode and the hydrogen concentration. Therefore, in order to estimate the hydrogen concentration we have used the constant K_{2100}, i.e., the well-established constant of the Si—H (s) mode. The greater electronegativity of carbon suggests that $K_{2140}>K_{2000}$. Therefore, the hydrogen concentration of this sample, i.e., $x=0.57$, is probably underestimated and so is the Si—C bond density.

---

*Present address: Penn State University, 275 Mat. Res. Lab., University Park, PA 16802-4801.

[1] J. Bullot and M. P. Schmidt, Phys. Status Solidi B **143**, 345 (1987).
[2] D. A. Anderson and W. E. Spear, Philos. Mag. **35**, 1 (1977).
[3] R. S. Sussmann and R. Ogden, Philos. Mag. B **44**, 137 (1981).
[4] D. R. McKenzie, J. Phys. D **18**, 1935 (1985).
[5] R. Rizzoli, R. Galloni, F. Demichelis, C. F. Pirri, E. Tresso, G. Crovini, P. Rava, and A. Madan, in *12th European Photovoltaic Solar Energy Conference*, edited by R. Hill, W. Palz, and P. Helm (H. S. Stephens & Associates, Bedford, UK, 1994), Vol. 1, p. 366.
[6] H. Wieder, M. Cardona, and C. R. Guarnieri, Phys. Status Solidi B **92**, 99 (1979).
[7] S. Pascarelli, F. Boscherini, S. Mobilio, and F. Evangelisti, Phys. Rev. B **45**, 1650 (1992).
[8] J. Tafto and F. J. Kampas, Appl. Phys. Lett. **46**, 949 (1985).
[9] M. A. Petrich, K. K. Gleason, and J. A. Reimer, Phys. Rev. B **36**, 9722 (1987).
[10] A. H. Mahan, B. von Roedern, D. L. Williamson, and A. Madan, J. Appl. Phys. **57**, 2717 (1985).
[11] C. Meneghini, S. Pascarelli, F. Boscherini, S. Mobilio, and F. Evangelisti, J. Non-Cryst. Solids **137&138**, 75 (1991).
[12] A. Chehaidar, R. Carles, A. Zwick, C. Meunier, B. Cros, and J. Durand, J. Non-Cryst. Solids **37**, 169 (1994).
[13] K. Mui, D. K. Basa, F. W. Smith, and R. Corderman, Phys. Rev. B **35**, 8089 (1987).
[14] Y. Catherine and G. Turban, Thin Solid Films **60**, 193 (1979).
[15] R. Galloni, R. Rizzoli, C. Summonte, F. Demichelis, F. Giorgis, C. F. Pirri, E. Tresso, G. Ambrosone, C. Catalanotti, U. Coscia, P. Rava, G. DellaMea, V. Rigato, A. Madan, and F. Zignani, in *Amorphous Silicon Technology—1994*, edited by E. A. Schiff, M. Hack, A. Madan, M. Powell, and A. Matsuda, MRS Symposia Proceedings No. 336 (Materials Research Society, Pittsburgh, 1994), p. 517.
[16] M. De Seta, S. L. Wang, F. Fume, and F. Evangelisti, Phys. Rev. B **47**, 7041 (1992).
[17] G. Wiech, W. Zahorowsky, and G. Weiser, J. Non-Cryst. Solids **114**, 483 (1989).
[18] G. Wiech, H. Langer, U. Lepa, and A. Simunek, J. Non-Cryst. Solids **164–166**, 1023 (1993).
[19] D. R. McKenzie, S. D. Berger, and L. M. Brown, Solid State Commun. **59**, 325 (1986).
[20] S. Pascarelli, F. Boscherini, S. Mobilio, and F. Evangelisti, Phys. Rev. B **45**, 1650 (1992).
[21] I. Solomon and L. Tessler, in *Amorphous Silicon Technology-1994* (Ref. 15), p. 505.
[22] G. B. Smith, D. R. McKenzie, and P. J. Martin, Phys. Status Solidi **152**, 475 (1989).
[23] F. Finochi and G. Galli, Phys. Rev. B **50**, 7393 (1994).
[24] P. Chaudhuri, S. Ray, A. K. Batabyal, and A. K. Barua, Thin Solid Films **121**, 233 (1984).
[25] E. Gat, B. Cros, R. Berjoan, and J. Durand, Appl. Surf. Sci. **64**, 345 (1993).
[26] J. Sotiropoulus and G. Weiser, J. Non-Cryst. Solids **97&98**, 1087 (1987).
[27] N. Saito, N. Tanaka, and I. Nakaaki, Appl. Phys. A **38**, 37 (1985).
[28] T. Shimada, Y. Katayama, and K. F. Komatsubara, J. Appl. Phys. **50**, 5530 (1979).
[29] A. Morimoto, T. Miura, M. Kumeda, and T. Shimizu, J. Appl. Phys. **53**, 7299 (1982).
[30] Y. Katayama, T. Shimada, and K. Usami, Phys. Rev. Lett. **46**, 1146 (1981).
[31] Y. Katayama, K. Usami, and T. Shimada, Philos. Mag. **43**, 283 (1981).
[32] Y. Inoue, S. Nakashima, A. Mitsushi, S. Tabata, and S. Tsuboi, Solid State Commun. **48**, 1071 (1983).
[33] A. Guivarc'h, J. Richard, and M. Le Contellec, J. Appl. Phys. **51**, 2167 (1980).
[34] N. Saito, T. Yamada, T. Yamaguchi, I. Nakaaki, and N. Tanaka, Philos. Mag. B, **52**, 987 (1985).
[35] S. Z. Han, H. M. Lee, and H. Kwon, J. Non-Cryst. Solids **170**, 199 (1994).

[36] A. Morimoto, T. Kataoka, M. Kumeda, and T. Shimizu, Philos. Mag. B **50**, 517 (1984).
[37] G. DellaMea, F. Demichelis, C. F. Pirri, P. Rava, V. Rigato, T. Stapinski, and E. Tresso, J. Non-Cryst. Solids **137&138**, 95 (1991).
[38] N. Saito, J. Appl. Phys. **59**, 2498 (1986).
[39] M. Katiyar, Y. H. Yang, and J. R. Abelson, J. Appl. Phys. **78**, 1659 (1995).
[40] D. R. McKenzie, G. B. Smith, and Z. Q. Liu, Phys. Rev. B **37**, 8875 (1988).
[41] M. Gorman and S. A. Solin, Solid State Commun. **15**, 761 (1974).
[42] T. Tohda, K. Wasa, and S. Hayakawa, J. Electrochem. Soc. **127**, 45 (1980).
[43] J. Robertson, Philos. Mag. B **66**, 615 (1992).
[44] F. W. Smith and Z. Yin, J. Non-Cryst. Solids **137&138**, 871 (1991).
[45] F. Evangelisti, J. Non-Cryst. Solids **164&166**, 1015 (1993).
[46] D. Engeman, R. Fisher, and J. Knecht, Appl. Phys. Lett. A **32**, 567 (1978).
[47] J. Roberston, J. Non-Cryst. Solids **198&200**, 615 (1996).
[48] S. E. Hicks, A. G. Fitzgerald, and S. H. Baker, Philos. Mag. B **62**, 193 (1990).
[49] T. Takeshita, Y. Kurata, and S. Hasegawa, J. Appl. Phys. **71**, 5395 (1980).
[50] F. Alvarez, M. Sebastiani, F. Pozzilli, P. Fiorini, and F. Evangelisti, J. Appl. Phys. **71**, 267 (1992).
[51] Y. Tawada, K. Tsudge, M. Kondo, H. Okamoto, and Y. Hamakawa, J. Appl. Phys. **53**, 5273 (1982).
[52] W. B. Jackson, N. M. Amer, A. C. Boccara, and D. Fournier, Appl. Opt. **20**, 1333 (1981).
[53] P. Rovira and F. Alvarez, Phys. Status Solidi B **192**, 535 (1995).
[54] R. Swanepoel, J. Phys. E **16**, 1214 (1983).
[55] See, for instance, Wei-Kan Chu, *Back Scattering Spectrometry* (Academic, New York, 1978).
[56] W. Beyer, J. Non-Cryst. Solids **97&98**, 1027 (1987).
[57] H. Wieder, M. Cardona, and C. R. Guarnieri, Phys. Status Solidi B **92**, 99 (1979).
[58] D. R. McKenzie, J. Phys. D **18**, 1935 (1985).
[59] F. Demichelis, G. Grovini, C. F. Pirri, E. Tresso, R. Galloni, R. Rizzoli, C. Summonte, F. Zignani, P. Rava, and A. Madan, Philos. Mag. B **69**, 377 (1994).
[60] M. Cardona, Phys. Status Solidi B **118**, 463 (1983).
[61] D. R. McKenzie, R. C. McPhedran, N. Savides, and L. C. Botten, Philos. Mag. B **48**, 341 (1983).
[62] K. Nakazawa, S. Ueda, M. Kumeda, A. Morimoto, and T. Shimizu, Jpn. J. Appl. Phys. **21**, L176 (1982).
[63] N. F. Mott and E. A. Davis, *Electronic Processes in Non-Crystalline Materials*, 2nd ed. (Clarendon, Oxford, 1979).
[64] S. S. Camargo, Jr. and W. Beyer, J. Non-Cryst. Solids **114**, 807 (1989).
[65] R. Zedlitz, E. Lotter, and M. Heintze, J. Non-Cryst. Solids **164&166**, 1031 (1993).
[66] R. C. Fang and L. Ley, Phys. Rev. B **40**, 3818 (1989).
[67] Y. Katayama, T. Shimada, L. Keisuke, and K. L. Kobayashi, Physica B **117B&118B**, 947 (1983).
[68] Y. Katayama, T. Shimada, T. Uda, and K. L. Kobayashi, J. Non-Cryst. Sol. **59&60**, 561 (1983).
[69] D. Wesner, S. Krummacher, R. Carr, T. K. Sham, M. Strongin, W. Eberhardt, S. L. Weng, G. Williams, M. Howells, F. Kampas, S. Head, and F. W. Smith, Phys. Rev. B **28**, 2152 (1983).
[70] F. Alvarez and L. R. Tessler, Solid State Phenom. **44–46**, 3 (1995).
[71] A. H. Mahan, P. Menna, and R. Tsu, Appl. Phys. Lett. **51**, 1167 (1987).
[72] M. De Seta, S. L. Wang, P. Narducci, and F. Evangelisti, J. Non-Cryst. Solids **137&138**, 851 (1991).
[73] M. Stutzman, Philos. Mag. B **60**, 531 (1989).
[74] A. A. Demkov and O. F. Sankey, Phys. Rev. B **48**, 2207 (1993).
[75] A. A. Langford, M. L. Fleet, B. P. Nelson, W. A. Landford, and N. Maley, Phys. Rev. B **45**, 13 367 (1992).
[76] B. K. Agrawal, P. S. Yadav, and B. K. Ghosh, Phys. Rev. B **39**, 7876 (1989).
[77] P. C. Kelires, Europhys. Lett. **14**, 43 (1991).
[78] J. Tersoff, Phys. Rev. B **49**, 16 349 (1994).